PHYSICAL REVIEW B VOLUME 55, NUMBER 5 1 FEBRUARY 1997-I

Ellipsometric measurement of the dielectric tensor of $Nd_{2-x}Ce_xCuO_{4-\delta}$

M. I. Alonso, S. Tortosa, M. Garriga, and S. Piñol
Institut de Ciència de Materials de Barcelona, CSIC, 08193 Bellaterra, Spain

(Received 2 May 1996; revised manuscript received 12 September 1996)

We study the anisotropic optical properties of a superconducting single crystal of $Nd_{2-x}Ce_xCuO_{4-\delta}$ ($x \simeq 0.16$). The two components of the dielectric tensor and its orientation with respect to the sample surface are obtained by analysis of ellipsometric data measured at room temperature from 1.4 to 5.1 eV. The optical anisotropy originates in the different spectral behavior of these two components. The ordinary dielectric function, which is related to the copper-oxygen planes, exhibits metallic character. The extraordinary component, related to excitations along the c axis, is nonmetallic and rather featureless. [S0163-1829(97)09405-8]

I. INTRODUCTION

The optical properties of cuprate-based high-T_c superconductors are strongly anisotropic due to their layered crystal structures. In particular, the unique electron-doped compounds $Nd_{2-x}Ce_xCuO_{4-\delta}$ have a tetragonal structure[1] (labeled T') where Cu atoms have a truly two-dimensional planar coordination.

Optical studies of these materials are mostly focused on reflectivity measurements in the far-infrared and midinfrared spectral regions[2–4] where the optical response is dominated by interesting free-carrier effects. For instance, the effects of sample reduction necessary to induce superconductivity, which are still not completely understood,[5] are investigated. Other essential pieces of information about the electronic structures of these materials are provided by measurements in the visible and near-uv energy regions. These measurements probe transitions between electronic states that, in these oxides, have orbital characters and are associated with specific local structures within the unit cell.[6] Detailed visible studies of electronic structure are useful for interpretation of resonant Raman scattering data.[7] Specifically, the values of the dielectric tensor are necessary to obtain absolute values of the electron-phonon coupling constants. Previous measurements of the reflectivity in different configurations have been performed in the $Pr_{2-x}Ce_xCuO_{4-\delta}$ system[8] over a wide energy region including the visible. However, no experimental values of the dielectric tensor of these materials are available in the literature.

In the present paper, we report on ellipsometric measurements of $Nd_{2-x}Ce_xCuO_{4-\delta}$ in the visible and near-uv region from 1.38 to 5.10 eV. Our main objective is to extract the two components of the dielectric tensor of this material. Recently, we have presented a method to do this in an anisotropic material without the need of having a well-oriented sample or knowing its orientation.[9] From our measurements we obtain both the magnitude of the dielectric tensor components and its orientation with respect to the sample surface. The observed spectral dependences correlate with the microscopic structure of the sample.

II. EXPERIMENTAL DETAILS

The single crystal used for this study was obtained by a self-flux method[10] and consisted of a 350-μm-thick platelet oriented in the plane perpendicular to the optical axis. To determine the tensor components, we took ellipsometric spectra in a polished side face of the crystal, which, under the optical Nomarski microscope, appeared very uniform and contained only very few small inclusions. For polishing we used successively finer diamond suspensions and a lubricant on suitable polishing cloths.[11] We finished with a 0.25-μm diamond suspension on a very soft and resilient cloth. After dismounting the sample from the wax, a thorough organic cleaning finished by a rinse in methanol was made. We have checked that this procedure gives good results for these materials. A final etching in Br-methanol solutions does not change the spectra significantly.

Measurements were done using a spectral ellipsometer with rotating polarizer[12] from 1.38 to 5.10 eV, at room temperature, and with the sample in ambient conditions. As-grown a-b surfaces appear to be very stable in these conditions. In contrast, we have observed that polished surfaces suffer a slow degradation, probably due to contamination of the surface favored by the residual damage induced by polishing. Therefore, a fresh optical-quality polish was done immediately before acquiring ellipsometric data. Since our light spot was larger than the sample surface (2×0.35 mm^2), we mounted the crystal so as to collect only the light reflected by the polished surface, and to discard the rest.

We studied the crystal both before and after reduction treatment. The optical spectra suggest a small compositional inhomogeneity of this crystal along the c axis, which is a usual problem with platelets thicker than ~70 μm. From our spectra, $x \simeq 0.16$ in the as-grown faces, whereas inside the crystal x tends to larger values. We will return to this point in Sec. IV. The crystal was reduced for 30 h in an Ar-rich atmosphere at 890 °C. We placed each surface of the platelet face up for 15 h, trying to reach a homogeneous reduction. The reduced sample was superconducting with a T_c onset at 19 K consistent with $x \simeq 0.16$ (Ref. 13). The superconducting transition was rather broad, also in agreement with the gradient of the Ce concentration, because the $T_c(x)$ decreases very steeply for $x > 0.16$. The observed compositional changes have very little influence on the absolute values of the dielectric functions, but the corresponding small variations are of the order of magnitude of those observed upon reduction. As a consequence, this sample is not quite suitable to study the reduction process, which has to be done in very homogeneous samples, such as ceramics or thinner single crystals, where in turn it is not possible to measure the dielectric tensor components. Therefore, here we concentrate on the study of the overall features of the dielectric tensor without considering the fine changes of ε related to the reduction process.

III. ANISOTROPIC MODEL

In this section, we give the basic equations used in this work and comment on their physical meaning. The described model is valid both for rotating analyzer ellipsometers (RAE's) and rotating polarizer ellipsometers (RPE's). Here, we discuss the case of measurements done with a RAE since the derivation of the equations is more straightforward. The final ellipsometric equations obtained in both cases are formally equivalent with some obvious substitutions as, for instance, the polarizer angle P by the analyzer angle A. In the experiment, the relevant measured quantities are $\tan\Psi$ and $\cos\Delta$ which describe the change of polarization state upon reflection, called complex reflectance ratio ρ (see, e.g., Ref. 14):

$$\rho=\frac{\chi_i}{\chi_r}=\tan\Psi e^{i\Delta}, \tag{1}$$

where χ_i and χ_r are the incident and reflected light polarization states, respectively.

For isotropic materials, $\rho=r_p/r_s$ coincides with the ratio between the Fresnel reflection coefficients for light polarized parallel, r_p, and perpendicular, r_s, to the plane of incidence. In this case the isotropic two-phase model applies and the complex dielectric function ε is only a function of ρ and the angle of incidence φ:

$$\varepsilon=\left(\frac{1-\rho}{1+\rho}\right)^2\tan^2\varphi\sin^2\varphi+\sin^2\varphi. \tag{2}$$

For anisotropic materials the relationship between measured ellipsometric parameters and sample properties is more complex. The general relationship between Jones vectors of incident $(E_{i,p},E_{i,s})$ and reflected $(E_{r,p},E_{r,s})$ light beams is given by[15,16]

$$\begin{pmatrix} E_{r,p} \\ E_{r,s} \end{pmatrix}=\begin{pmatrix} r_{pp} & r_{ps} \\ r_{sp} & r_{ss} \end{pmatrix}\begin{pmatrix} E_{i,p} \\ E_{i,s} \end{pmatrix}, \tag{3}$$

where the mixing of s and p polarizations upon reflection is represented by the nondiagonal reflection matrix. The elements of the reflection matrix depend only on φ and on the components of the dielectric tensor of the material and its orientation relative to the sample surface. Using Eq. (3), incident and reflected polarization states are related by

$$\chi_r=\frac{(r_{sp}/r_{ss})+\chi_i}{(r_{pp}/r_{ss})+(r_{ps}/r_{ss})\chi_i}. \tag{4}$$

By analogy with the isotropic case we define now the complex pseudoreflectance ratio $\langle\rho\rangle=\chi_i/\chi_r$. With this definition, Eq. (4) can be rewritten as

$$\langle\rho\rangle=\frac{(r_{pp}/r_{ss})+(r_{ps}/r_{ss})\tan P}{1+(r_{sp}/r_{ss})(\tan P)^{-1}}, \tag{5}$$

where we have introduced that the incident linear polarization state $\chi_i=\tan P$ is determined by the angle azimuth P of the fixed polarizer. Obviously, the pseudodielectric function $\langle\varepsilon\rangle$ inferred from $\langle\rho\rangle$ in the isotropic two-phase model [Eq. (2)] depends on P. This must be borne in mind when measured data are represented as $\langle\varepsilon\rangle$.

To obtain the dielectric tensor we solve numerically the exact ellipsometric equations using the 4×4 technique developed by Yeh[15] and implemented as described in Ref. 16. In a uniaxial material the dielectric tensor has two independent components, the ordinary ε_o and extraordinary ε_e. The orientation of the optic axis is given by the two Euler angles α and β, where α is the angle between the optic axis and the surface normal $(0\leqslant\alpha\leqslant 90°)$ and β is the angle between the projection of the optic axis onto the sample surface and the normal to the plane of incidence $(0\leqslant\beta<360°)$. By measuring various spectra at different β values, and using a least-squares-fitting procedure energy by energy, we find the $\varepsilon_o(\omega)$ and $\varepsilon_e(\omega)$ that better represent all measured data.

The dependence on P given by Eq. (5) vanishes for specific orientations of the dielectric tensor, that is, when no mixing between s and p polarization can occur so that $r_{sp}=0=r_{ps}$ and $\langle\rho\rangle=r_{pp}/r_{ss}$. In a uniaxial material these special cases happen whenever the optic axis is contained in the plane of incidence or is perpendicular to it. The values of Euler angles that fulfill these conditions are the following: The optic axis is in the plane of incidence when $\alpha=0$ (*a*-*b* plane) or when $\beta=90°,270°$. The perpendicular situation occurs when $\alpha=90°$ and $\beta=0,180°$. The properties of these particular orientations allow us to find readily the orientation of the dielectric tensor and therefore of the crystal by measuring at most two β scans at two different polarizer angles.[9] For the mentioned orientations the spectra are independent of P but strictly the measured $\langle\rho\rangle$ or the calculated $\langle\varepsilon\rangle$ have no direct physical interpretation, even in the particular case $\alpha=0$ where the sample behaves as isotropic.[17] However, in many cases, the representation of measured data as $\langle\varepsilon\rangle$ gives a physically intuitive view.[18]

There is no simple recipe to find an optimum P angle, in terms, for instance, of maximizing the anisotropic optical response, to make the measurements. From Eq. (5) we see that the polarization mixing terms become most important near $P=0,90°$. But these values are not usually the best choices to obtain spectra with a good signal-to-noise ratio or best precision.[19] In practice, a compromise between maximum anisotropy and favorable measurement conditions must be found. In any case, simulations with approximate ε values are useful and give the correct qualitative tendencies.

IV. RESULTS

A. Spectral behavior of ε

In the first place, we anticipate some results aiming mainly at characterization of the studied crystal. Since thick platelets are likely to have inhomogeneous composition, we checked optically this possibility: The intensity and energy position of the observed spectral features correlate with the composition of the sample. Ellipsometric spectra taken at

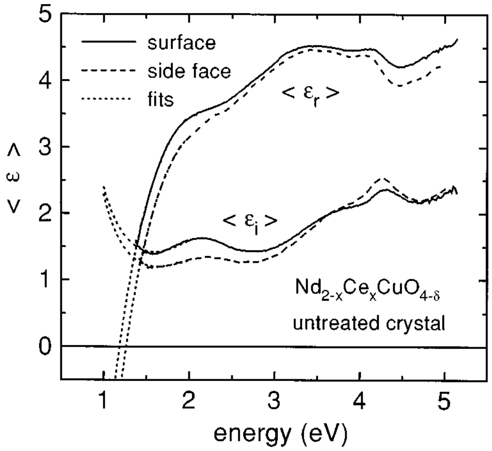

FIG. 1. Comparison of pseudodielectric functions $\langle\varepsilon\rangle$ measured in the nontreated $Nd_{2-x}Ce_xCuO_{4-\delta}$ crystal. Both $\langle\varepsilon\rangle$ spectra correspond to *a*-*b* planes. Data obtained from direct measurement on the as-grown *a*-*b* surfaces are plotted with solid lines. Dashed lines correspond to data computed from the dielectric tensor elements measured on the polished side face. Dotted lines are calculated from fits to the data below 2.5 eV by using Eq. (6).

both as-grown surfaces of the platelet did not indicate appreciable differences in composition. On the contrary, the measurements done in the polished side face denote composition differences between this and the as-grown surfaces. In Fig. 1 we compare their respective ellipsometric spectra displayed as pseudodielectric functions related to *a*-*b* planes. The spectrum assigned to the polished side face is calculated from the measured dielectric tensor components, which are not shown. Although these $\langle\varepsilon\rangle$ are not the correct dielectric functions, they contain the spectral features associated to *a*-*b* planes and, in any case, their direct comparison is meaningful.

The dielectric response of *a*-*b* planes in this energy range exhibits three characteristic spectral features: Two distinct electronic transitions near 2 eV and 4.3 eV, and a Drude-type behavior at energies below ~2.5 eV. The latter is well represented by a Drude-Lorentz line shape:[20]

$$\varepsilon(E)=\varepsilon_\infty-\frac{E_p^2}{E(E+i\Gamma)}+\frac{F}{E_0^2-E(E+i\gamma)}, \qquad (6)$$

where ε_∞ describes high-energy contributions, E_p is the unscreened plasma energy of the free carriers, and Γ is their scattering rate. The screened plasma energy $E_p/\sqrt{\varepsilon_\infty}$ corresponds to the energy of the free-carrier plasma oscillations and coincides with the zero crossing of the real part ε_r, provided the Lorentz term in Eq. (6) is negligible at that energy. The Lorentz term centered at E_0 and broadened by γ represents the contribution of interband transitions within the considered energy range. We find the precise energies of the higher electronic transitions from fits to the numeric second-derivative spectra by using theoretical Lorentzian line shapes.

The peak near 2 eV is reminiscent of the charge-transfer (CT) transition that takes place in undoped Nd_2CuO_4 at about 1.6 eV.[21,22] The microscopic origin of this peak and its change upon carrier doping has been explained by calculations of the one-particle excitation spectra using finite-size clusters.[23] In this model, the CT transition occurs between the occupied Zhang-Rice singlet band (O 2*p* states) and the empty upper Hubbard band (Cu $3d_{x^2-y^2}$ states). By doping, the energy of this transition increases whereas its intensity is reduced due to reconstruction of spectral weights in both these bands.[23] The results of band structure calculation of Szotek *et al.*[24] with the linear-muffin-tin-orbital (LMTO) method also show that electronic excitations in this energy range must be due to transitions involving electronic states in the CuO_2 planes. We now turn to the much less studied higher-energy structure that is seen at about 5.5 eV in Nd_2CuO_4 and at 4.3 eV in our doped sample. To assign correctly this structure the cluster model is insufficient because the final states are most likely related to Cu 4*s* states.[8] The LMTO band structure[24] shows that possible final states in the correct energy range can include important hybridization from Nd *d* bands. Cerium doping pushes down the unoccupied Nd *d* bands by about 1 eV, and hence this may contribute to the observed change in transition energy. However, this is speculative and a calculation of the interband contributions to the imaginary part of ε would be necessary to make an assignment. By similarity with other compounds, it has been suggested that this optical feature can be a signature of the presence of Cu^+ in the doped compound.[6] Indeed, the LMTO calculated effective charges on the Cu sites indicate a reduction of positive charge upon Ce doping.

By comparing the spectra displayed in Fig. 1, relevant differences in the three aforementioned spectral features are apparent. Notice that, in view of the small penetration depth of light in the material ($<1\mu$m), this indicates differences between the local compositions of the surfaces and the inner part of the sample. All differences observed in Fig. 1 point in the same direction, namely, a higher carrier concentration inside the sample than in the as-grown surfaces. This is clearly indicated by a higher plasma energy in the dashed-line spectrum and is consistent with the evident concomitant decrease of the intensity of the peak near 2 eV.[3] Also, the 4.3-eV peak occurs at lower energy in the dashed-line spectrum than in the solid-line spectrum. We have calibrated the energy position of this peak as a function of x in untreated $Nd_{2-x}Ce_xCuO_{4-\delta}$ samples, both ceramics and single crystals with known x concentrations. Assuming that the O content is homogeneous and attributing the observed differences to changes in Ce content only, the peak energies indicate that $x\simeq0.16$ in the as-grown faces, while x is larger inside the crystal. From these measurements we cannot distinguish if the crystal has a graded composition or, for instance, Ce-depleted surfaces. From the known growth mechanism of stepwise formation of *a*-*b* layers from the liquid flux,[10] the first possibility seems more likely. From our results we estimate this gradient of Ce concentration to be less than 4%.

From the optical point of view, the reduction treatment diminishes the observed compositional inhomogeneity. We believe this is due to an homogeneization of the carrier concentration whose origin may be an incomplete reduction process. It can also be explained if the quantity of reduced O depends on x and is larger for $x=0.16$ than for $x=0.20$. We have observed the latter effect in homogeneous ceramic samples. In Fig. 2, the improved homogeneity of the reduced sample from the optical point of view is evidenced by the smaller differences between both shown spectra. Although

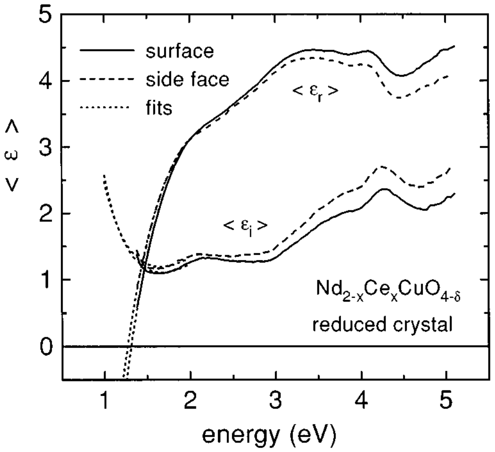

FIG. 2. Similar data as in Fig. 1 but obtained after the reduction treatment.

the $\langle \varepsilon \rangle$ values differ somewhat, especially in the uv spectral region, the relevant spectral features occur at the same or very close energies. The discrepancy in absolute $\langle \varepsilon \rangle$ values can be caused partly by imperfect surface quality or slight contamination of the polished surface.

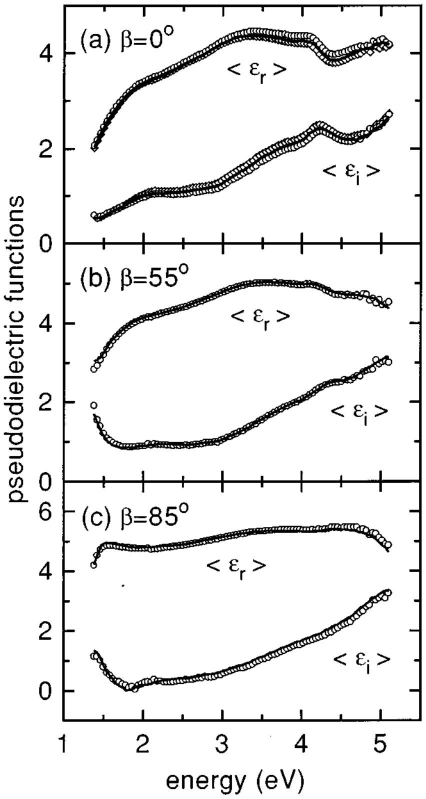

FIG. 3. Pseudodielectric functions $\langle \varepsilon \rangle$ obtained at three different β values on the polished side face of the reduced $Nd_{2-x}Ce_xCuO_{4-\delta}$ crystal. Symbols display measured data, and lines are calculated from the fitted tensor components shown in Fig. 4. (a) $\beta = 0°$. The difference between the two plotted data sets shows the slow degradation of the polished surface. The spectrum plotted with circles was the first, the one with lozenges the last of the series. (b) $\beta = 55°$. (c) $\beta = 85°$. Notice the different vertical scales.

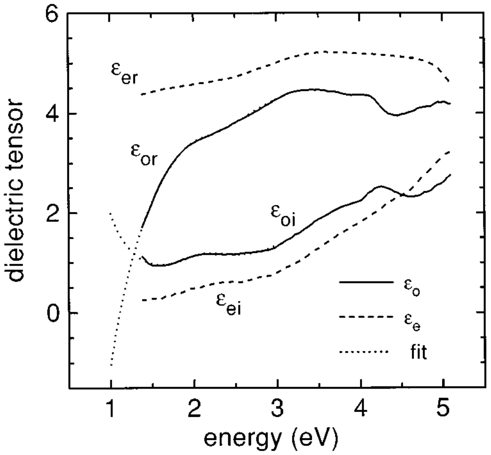

FIG. 4. Dielectric functions of the reduced $Nd_{2-x}Ce_xCuO_{4-\delta}$ crystal. ε_o denotes the ordinary component and ε_e the extraordinary one. The dotted lines are calculated from Eq. (6) with our fitted parameters (see text).

B. Study of the anisotropy

Next, we present in detail the anisotropy study for the reduced sample. Following the method described in Ref. 9, we first determined the orientation of the polished surface by measuring two β scans at the two fixed analyzer angles of 7° and 20°. These measurements were done in the region of largest optical anisotropy at the fixed energy of 1.505 eV, close to a line of the Xe lamp. The orientation of the polished surface found from the fit was $\alpha = 80.4° \pm 0.5°$. This value coincided with the angle between this and the as-grown *a-b* surface measured directly using a microscope. Once the orientation is known, to extract the spectral dependence of the dielectric tensor we took ellipsometric spectra at 25 different β values. The spectra were taken from 1.38 to 5.10 eV in steps of 0.04 eV. All spectra were measured at $\varphi = 65°$ and $A = 20°$. The anisotropic sample properties are illustrated in Fig. 3, where we show spectra measured at three different β azimuths of the sample, together with simulations using the fitted tensor components displayed in Fig. 4. The value $\beta = 0°$ was measured twice. We included both data sets shown in Fig. 3(a) in the fitting procedure to obtain $\varepsilon(\omega)$. The measurements of *a-b* faces were not taken into account due to the observed difference in composition. The values where $\langle \varepsilon_i \rangle \sim 0$ in Fig. 3(c) around 1.7 eV have the largest experimental errors, due to uncertainty in the measurement of $\cos\Delta$.

Figure 4 shows our main result: the dielectric tensor components of the reduced crystal. It is apparent from this figure that the optical anisotropy arises from the different character of the two components. The extraordinary component ε_e displays nonmetallic behavior and is rather featureless in this energy range. The ordinary dielectric function ε_o reflects the metallic character of the *a-b* copper-oxygen planes. In its real part, ε_{or}, the Drude contribution influences the whole spectrum and dominates the range below ~ 2.5 eV. The parameters of the fitted Drude-Lorentz dielectric function [see Eq. (6)] displayed in Fig. 4 by dotted lines are $\varepsilon_\infty = 5.0 \pm 0.3$, $E_p = 2.5 \pm 0.3$ eV, $\Gamma = 0.2 \pm 0.1$ eV, $F = 1.0 \pm 0.5$ eV^2,

$E_0 = 2.2 \pm 0.1$ eV, and $\gamma = 1.0 \pm 0.2$ eV. The value of ε_∞ is reduced from 5.0 to 2.9 if we include explicitly a higher-energy electronic contribution around 4 eV, but the other parameters remain unchanged within their respective error bars. The value $\varepsilon_\infty = 2.9$ is an upper limit to the *true* ε_∞. The good agreement between measurement and fit is remarkable. The resultant Drude parameters resemble those found for $YBa_2Cu_3O_7$ from ellipsometric measurements in the near ir region.[20]

In order to compare our results with available reflectivity (R) measurements in these materials we have calculated the normal-incidence reflectivity from the tensor components shown in Fig. 4. Results are shown in Fig. 5. For the configuration $E \| c$ we compare our measurement with that done by Arima *et al.*[8] in the related compound $Pr_{1.85}Ce_{0.15}CuO_{4-\delta}$. The reflectivity of both systems has similar spectral behavior and quite close values of R are obtained. For the usually measured $E \perp c$ configuration, we have extrapolated down to 1 eV by using our fitted Drude-Lorentz dielectric function. As is shown in Fig. 5, our result closely coincides with the measurement by Lupi *et al.*[3] for $Nd_{1.83}Ce_{0.17}CuO_{4-\delta}$ in the overlap range 1–2.4 eV. In addition, this excellent agreement even with the extrapolated reflectivity confirms the reliability of our fitting procedure to represent the ε_o of these materials in the near ir region. There is only qualitative agreement with the measurement on the $Pr_{1.85}Ce_{0.15}CuO_{4-\delta}$ crystal:[8] The spectral behaviors are the same but the reflectivity values do not coincide, especially, in the region of the plasma minimum.

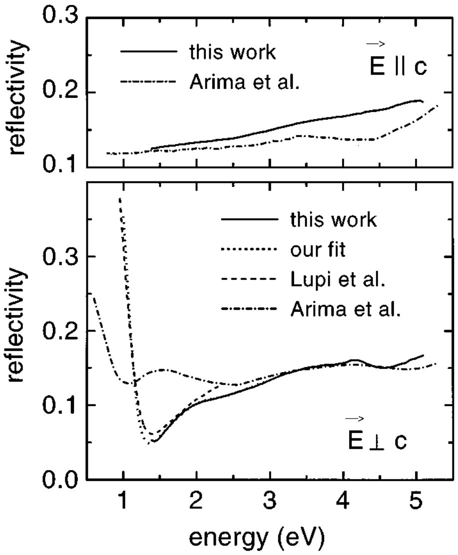

FIG. 5. Normal-incidence reflectivities in the two possible configurations: $E \| c$ (upper panel) and $E \perp c$ (lower panel). Solid and dotted lines are calculated from the tensor components given in Fig. 4. Dashed and dash-dotted lines represent, respectively, reflectivity measurements on $Nd_{1.83}Ce_{0.17}CuO_{4-\delta}$ (Ref. 3) and $Pr_{1.85}Ce_{0.15}CuO_{4-\delta}$ (Ref. 8).

V. SUMMARY

By applying an experimental approach, we have determined the dielectric tensor of a single crystal of $Nd_{2-x}Ce_xCuO_{4-\delta}$ ($x \simeq 0.16$) from 1.38 to 5.10 eV at room temperature. Both the two independent components of $\varepsilon(\omega)$ and the orientation of this tensor with respect to the sample surface have been measured. The ordinary component, related to the copper-oxygen planes, contains characteristic interband transitions and exhibits metallic character with a screened plasma energy of 1.1 eV. The extraordinary component shows nonmetallic behavior without associated transitions in the studied energy range.

ACKNOWLEDGMENTS

This work has been supported by the Spanish CICYT Project No. MAT94-1336 and the EU Project TOPHIGHTS (No. CIPA–CT93–0032). One of the authors (S.T.) wishes to thank the DGR (Generalitat de Catalunya) for support. We are thankful to A. Gou for the T_c measurement.

---

[1] Y. Tokura, H. Tokagi, and S. Uchida, Nature **337**, 345 (1989).

[2] E. V. Abel', V. S. Bagaev, D. N. Basov, O. V. Dolgov, A. F. Plotnikov, A. G. Poiarkov, and W. Sadowski, Solid State Commun. **79**, 931 (1991).

[3] S. Lupi, P. Calvani, M. Capizzi, P. Maselli, W. Sadowski, and E. Walker, Phys. Rev. B **45**, 12 470 (1992).

[4] R. A. Hughes, Y. Lu, T. Timusk, and J. S. Preston, Phys. Rev. B **47**, 985 (1993).

[5] M. Brinkmann, T. Rex, H. Bach, and K. Westerholt, Phys. Rev. Lett. **74**, 4927 (1995).

[6] M. K. Kelly, P. Barboux, J.-M. Tarascon, and D. E. Aspnes, Phys. Rev. B **40**, 6797 (1989).

[7] E. T. Heyen, R. Liu, M. Cardona, S. Piñol, R. J. Melville, D. McK. Paul, E. Morán, and M. A. Alario-Franco, Phys. Rev. B **43**, 2857 (1991).

[8] T. Arima, Y. Tokura, and S. Uchida, Phys. Rev. B **48**, 6597 (1993).

[9] M. I. Alonso, M. Garriga, F. Alsina, and S. Piñol, Appl. Phys. Lett. **67**, 596 (1995).

[10] S. Piñol, J. Fontcuberta, C. Miravitlles, and D. McK. Paul, Physica C **165**, 265 (1990).

[11] DP-Products (Diamond Sprays, Blue Lubricant and Cloths) supplied by Struers, Copenhagen, Denmark.

[12] Model ES4G, manufactured by SOPRA, Bois-Colombes, France.

[13] J. Fontcuberta and L. Fàbrega, in *Studies on High Temperature Superconductors*, edited by by A. V. Narlikar (Nova Science Publishers, New York, 1996), Vol. 16.

[14] R. M. A. Azzam and N. M. Bashara, *Ellipsometry and Polarized Light* (North-Holland, Amsterdam, 1987).

[15] P. Yeh, Surf. Sci. **96**, 41 (1980).

[16] M. Garriga, Ph.D. thesis, University of Stuttgart, 1990.

[17] D. J. De Smet, J. Appl. Phys. **76**, 2571 (1994).

[18] D. E. Aspnes, J. Opt. Soc. Am. **70**, 1275 (1980).

[19] D. E. Aspnes, J. Opt. Soc. Am. **64**, 639 (1974).

[20] J. Humlíček, J. Kircher, H.-U. Habermeier, M. Cardona, Y. Fang, U. Welp, K. Vanderwoort, and D. Crabtree, Solid State Commun. **79**, 673 (1991).

[21] S. L. Cooper, G. A. Thomas, A. J. Millis, P. E. Sulewski, J. Orenstein, D. H. Rapkine, S.-W. Cheong, and P. L. Trevor, Phys. Rev. B **42**, 10 785 (1990).

[22] T. Arima, K. Kikuchi, M. Kasuya, S. Koshihara, Y. Tokura, T. Ido, and S. Uchida, Phys. Rev. B **44**, 917 (1991).

[23] T. Yohyama and S. Maekawa, Physica C **191**, 193 (1992).

[24] Z. Szotek, G. Y. Guo, and W. M. Temmerman, Physica C **175**, 1 (1991).